



**HAL**  
open science

# Iodine uptake in brown seaweed exposed to radioactive liquid discharges from the reprocessing plant of ORANO La Hague

Bruno Fiévet, Claire Voiseux, Catherine Leblanc, Denis Maro, Didier Hebert, Luc Solier, Claire Godinot

## ► To cite this version:

Bruno Fiévet, Claire Voiseux, Catherine Leblanc, Denis Maro, Didier Hebert, et al.. Iodine uptake in brown seaweed exposed to radioactive liquid discharges from the reprocessing plant of ORANO La Hague. *Journal of Environmental Radioactivity*, 2023, 256, pp.107045. 10.1016/j.jenvrad.2022.107045 . hal-03873915

**HAL Id: hal-03873915**

**<https://hal.sorbonne-universite.fr/hal-03873915>**

Submitted on 3 Jul 2023

**HAL** is a multi-disciplinary open access archive for the deposit and dissemination of scientific research documents, whether they are published or not. The documents may come from teaching and research institutions in France or abroad, or from public or private research centers.

L'archive ouverte pluridisciplinaire **HAL**, est destinée au dépôt et à la diffusion de documents scientifiques de niveau recherche, publiés ou non, émanant des établissements d'enseignement et de recherche français ou étrangers, des laboratoires publics ou privés.



Distributed under a Creative Commons Attribution - NonCommercial - NoDerivatives 4.0 International License

# Iodine uptake in brown seaweed exposed to radioactive liquid discharges from the reprocessing plant of ORANO La Hague

FIEVET Bruno<sup>a</sup>, VOISEUX Claire<sup>a</sup>, LEBLANC Catherine<sup>b</sup>, MARO Denis<sup>a</sup>, HEBERT Didier<sup>a</sup>, SOLIER Luc<sup>a</sup>, GODINOT Claire<sup>a\*</sup>

<sup>a</sup>Institut de Radioprotection et de Sûreté Nucléaire, PSE-ENV/SRTE, Laboratoire de Radioécologie de Cherbourg-Octeville, France

<sup>b</sup>Sorbonne Université, CNRS, UMR 8227, Integrative Biology of Marine Models, Station Biologique de Roscoff, Roscoff, France

\* corresponding author

Claire GODINOT. IRSN, Laboratoire de Radioécologie, Rue Max Pol Fouchet, BP10, 50130 Cherbourg-en-Cotentin, France.

[claire.godinot@irsn.fr](mailto:claire.godinot@irsn.fr).

## Abstract

Iodine-129 is present in controlled liquid radioactive waste routinely released in seawater by the ORANO nuclear fuel reprocessing plant in La Hague (Normandy, France). Brown algae are known for their exceptional ability to concentrate iodine from seawater. They also potentially emit volatile iodine compounds in response to various stresses, such as during emersion at low tide. For these reasons, brown seaweed is routinely collected for radioactivity monitoring in the marine environment. Despite the high concentration ratio the exact mechanism of iodine uptake is still unclear. Chemical imaging by laser desorption/ionization mass spectrometry provided evidence that iodine is stored by kelps as I<sup>-</sup>. In this study we investigate *in vivo* iodine uptake in kelps (*Laminaria digitata*) with an emphasis on seawater iodine chemical speciation. Our results showed that kelp plantlets were able to take up iodine in the forms of both IO<sub>3</sub><sup>-</sup> and I<sup>-</sup>. We also observed transient net efflux of I<sup>-</sup> back to seawater but no IO<sub>3</sub><sup>-</sup> efflux. Since the seaweed stores I<sup>-</sup> but takes up both IO<sub>3</sub><sup>-</sup> and I<sup>-</sup>, IO<sub>3</sub><sup>-</sup> was likely to be converted into I<sup>-</sup> at some point in the plantlet, or through the action of associated microorganisms. One major outcome of our experiments was the direct observation of the kelp-based biogenic conversion of seawater IO<sub>3</sub><sup>-</sup> into I<sup>-</sup>. On the basis of both IO<sub>3</sub><sup>-</sup> and I<sup>-</sup> uptakes by the seaweed, we propose new steps in the possible iodine concentration mechanism used by kelp.

Keywords: radioactive iodine, uptake, kelp, chemical speciation

## 1 Introduction

Though a minor element in seawater, iodine is mainly present on Earth dissolved in the oceans (Carpenter, 2003; Carpenter et al, 2021; Chance et al, 2014; Wong, 1991). In the terrestrial environment, it is present at very low levels in soils, water and plants, but in vertebrates, it is involved in the crucial functions of the thyroid gland as organically bound in thyroid hormones (Fuge & Johnson, 2015). Iodine is also present as multiple volatile compounds involved in a complex geochemical cycle between the oceans and the atmosphere. The high reactivity of iodine is considered to play a key role in atmospheric chemistry and possibly the climate, at least in coastal environments (Carpenter et al, 2021; Carpenter et al, 2013; Kolb, 2002; Saiz-Lopez et al, 2012). In addition to stable <sup>127</sup>I, iodine has 36 radioactive isotopes, and with the exception of <sup>129</sup>I (half-life of 15.7 10<sup>6</sup> years), most iodine radioisotopes quickly decay (half-lives of a few days). Two main iodine radioisotopes are generated by

42 human activities.  $^{131}\text{I}$  is a short-lived (half-life of 8.5 days) fission by-product of  $^{235}\text{U}$  in nuclear electricity  
43 production, and high activities are also used in medicine for cancer radiotherapy.  $^{129}\text{I}$  is generated in  
44 nuclear reactors, and because of its very slow decay rate, it is a major residual iodine radioisotope in  
45 the nuclear fuel cycle, which adds to naturally occurring  $^{129}\text{I}$  (cosmic ray spallation of Xe in the  
46 atmosphere and spontaneous fission of natural uranium). It is also present in fallout from past  
47 atmospheric nuclear weapons testing and major powerplant accidents.  $^{129}\text{I}$  is present in controlled  
48 liquid radioactive waste routinely released in seawater by the ORANO nuclear fuel reprocessing plant  
49 in La Hague (Normandy, France) and the annual amounts released are between 1 and 2 TBq.yr<sup>-1</sup> (Fiévet  
50 et al, 2020). Discharging liquid  $^{129}\text{I}$  waste into seawater results in isotopic dilution in naturally-present  
51 stable  $^{127}\text{I}$ . The background isotopic ratio  $^{129}\text{I}/^{127}\text{I}$  is in the range  $[10^{-13}-10^{-12}]$  and reaches  $[10^{-7}-10^{-6}]$  in  
52 seawater in the English Channel (Hou et al, 2007). Considering a concentration of dissolved  $^{127}\text{I}$  in  
53 seawater of 0.5  $\mu\text{M}$ , this means  $^{129}\text{I}$  activities in the range  $[0.05-0.5]$  Bq.m<sup>-3</sup>. However, higher seawater  
54  $^{129}\text{I}$  activities could be expected in the close vicinity of the ORANO plant outlet.

55 Brown algae are known for their exceptional ability to concentrate iodine from seawater. The ratio  
56 of iodine content between kelps (i.e. Laminariales) and seawater reaches  $10^5$ , especially in young  
57 plantlets (Leblanc et al, 2006). Moreover, brown algae are also known to release volatile iodine  
58 compounds in response to various stresses, such as during emersion at low tide (Ball et al, 2010;  
59 McFiggans et al, 2010; McFiggans et al, 2004; O'Dowd et al, 2002; Whitehead et al, 2009). Wherever  
60 brown seaweed is exposed to  $^{129}\text{I}$  discharges in seawater, the radioisotope could return to the  
61 terrestrial environment via an airborne route, namely via the wind and aerosols. For these reasons,  
62 brown seaweed is routinely collected in the marine environment in the English Channel to monitor  
63 radionuclide concentrations, and in particular that of  $^{129}\text{I}$  (Fiévet et al, 2020). In a previous study on  
64 radionuclide transfers between seawater and biota, we observed that the bioavailability of  $^{129}\text{I}$   
65 appeared to decrease with distance from the source of input (the ORANO La Hague plant outlet). We  
66 emphasized the role of the chemical speciation of dissolved iodine in seawater (Fiévet et al, 2021).  
67 Iodine uptake by Laminariales, and more generally brown algae, is hypothesized to be mediated by  
68 enzymes from the vanadium-haloperoxidase (VHPO) family, through the specific oxidation of iodide  
69 (Küpper et al, 1998). Dissolved iodine is naturally present in seawater in the forms of iodide ( $\text{I}^-$ ) and  
70 iodate ( $\text{IO}_3^-$ ). Although iodate is the dominant chemical form because of pH and redox potential in  
71 seawater, both chemical forms are present in various proportions (Carpenter et al, 2013; Hou et al,  
72 2007; Wong, 1991). The conversion mechanisms between iodine species are still unclear because  
73 iodate does not spontaneously reduce to iodide in natural seawater for thermodynamic reasons (Hou  
74 et al, 2007). Nevertheless this reaction between iodate and iodide takes time to reach equilibrium  
75 (Luther et al, 1995), around two weeks according to estimates (Carpenter, pers. Comm.). Now,  
76 depending on the chemical form of  $^{129}\text{I}$  discharged by the reprocessing plant, the question arises as to  
77 its bioavailability for seaweed. The PUREX process  
78 (<https://www.cea.fr/Documents/monographies/Procédé-PUREX.pdf>) operated at the ORANO  
79 reprocessing plant results in the liquid release of  $^{129}\text{I}$  as iodide. As such, it is assumed to be a potential  
80 substrate for VHPOs, being incorporated by kelps. But as conversion into  $^{129}\text{IO}_3^-$  occurs in seawater, it  
81 may become unavailable for the enzyme. In summary, two crucial questions should be answered to  
82 better understand  $^{129}\text{I}$  uptake by brown seaweed in the marine environment around the reprocessing  
83 plant of ORANO La Hague: 1- Which form of iodine is bioavailable for uptake by brown seaweed? 2-  
84 Does it evolve with time and distance from the outlet once released in seawater by the plant? More  
85 generally, the exact mechanism of iodine uptake is still unclear, and was challenged by chemical  
86 imaging results confirming a major apoplastic storage location (Lebeau et al, 2021). Assessing which  
87 chemical form of seawater iodine is taken up by kelps in the marine environment should contribute to  
88 the exploration of its bioaccumulation mechanism.

89 In this study, we investigate *in vivo* iodine uptake in *L. digitata* with an emphasis on chemical  
90 speciation between iodide vs iodate. We also use radioactive  $^{131}\text{I}^-$  as a tracer of unidirectional iodide  
91 influx to estimate iodide turnover in seaweed as well as the relationship with seawater iodide  
92 concentration. We also report an isotopic ratio  $^{129}\text{I}/^{127}\text{I}$  measured in the marine environment in the  
93 vicinity of the outlet of the ORANO reprocessing plant in La Hague. Iodine-129 activity and stable iodine  
94 concentrations were determined in total dissolved iodine in seawater and as total iodine extracted  
95 from two species of brown seaweed, *L. digitata* and *Fucus serratus* collected in Goury (6 Km from the  
96 plant outlet). Finally, laboratory experiment results and data from the natural environment are put  
97 into perspective to attempt to better understand radioactive iodine transfers between seawater and  
98 brown seaweed.

## 99 2 Material and methods

### 100 2.1 Algal material

101 For iodine uptake experiments, plantlets of *Laminaria digitata* [0.05-3 g] were collected on the  
102 rocks in Goury (Normandy, France) at low tide (spring-tides) and transferred to the laboratory (LRC,  
103 IRSN, Cherbourg, France) for maintenance in an aquarium. The temperature was set to that of the  
104 natural environment upon collection (12.5 °C), the water was aerated and recirculated. About 200 g of  
105 total biomass (plantlets and young sporophytes, see below) was kept in a 60 L tank in natural light, and  
106 the seawater was replaced every week with pre-cooled fresh seawater. The iodine concentration in  
107 seawater (see 2.2.2) was checked to ensure no depletion occurred.

108 For  $^{131}\text{I}$  experiments, we used both whole plantlets and tissue disks. In the latter case, disks of about  
109 0.04-0.05 g (diam. 14 mm) were punched out of the blade of young sporophytes (20-40 cm long;  
110 collected and maintained as described above) of *L. digitata* by die-cutting. Algal disks were then kept  
111 in filtered seawater (seawater collected in Goury, filtered at 0.45  $\mu\text{m}$ ; Millipore ref. HAWG0700) until  
112 iodine leakage stopped, as indicated by the monitoring of iodine concentration in seawater (with one  
113 disk in 10 mL of seawater: no iodine leakage was observed after 1 hour).

114 For the environmental monitoring of  $^{129}\text{I}/^{127}\text{I}$ , adult sporophytes of *L. digitata* (1-1.5 m in length)  
115 and *Fucus serratus* (30-70 cm in length) were collected monthly at low tide at Goury for 37 months  
116 (see supplementary material S2-1 for sampling location).

### 117 2.2 Determination of $\text{I}^-$ and $\text{IO}_3^-$ in seawater

#### 118 2.2.1 Separation of seawater $\text{I}^-$ and $\text{IO}_3^-$

119 After sample filtration (0.45  $\mu\text{m}$ , Millipore ref. HAWG0700), seawater  $\text{I}^-$  and  $\text{IO}_3^-$  were separated by  
120 anion exchange chromatography (AEC) using Bio-Rad AG1-X4 resin and mini-spin columns according  
121 to (Hou et al, 2001; Zhang, 2015). Briefly, AG1-X4 resin (provided in  $\text{Cl}^-$  form) was conditioned into  $\text{NO}_3^-$   
122 form as follows: 1- a first wash in  $\text{NaClO}$  5% removed any residual  $\text{I}^-$  from the fresh resin. 2-  $\text{Cl}^-$  was  
123 replaced by  $\text{NO}_3^-$  in  $\text{NaNO}_3$  2M. 3- Excess  $\text{NO}_3^-$  was finally flushed with MilliQ water (Millipore). About  
124 0.5 cc of conditioned resin ( $\text{NO}_3^-$  form) was added to mini Bio-spin columns (Bio-Rad #7326207) and  
125 allowed to drain by gravity. Then 3 more 0.9 mL washes of MilliQ water were applied and left to drain  
126 prior to starting AEC on filtered (0.45  $\mu\text{m}$ ) seawater as follows: 1- two 0.9 mL seawater samples were  
127 passed through the resin to replace the mobile phase. 2- The bottom of the column was closed with  
128 the stopper tip, another 0.9 mL sample was added and the top was closed with the cap. The column  
129 was flipped twice and agitated horizontally for 1 hour on a 3D-platform shaker (Polymax) at slow  
130 speed. 3- The bottom stopper tip and the top cap were removed and the mobile phase was allowed to  
131 drain in a 1.5 mL centrifuge tube. The flow-through contained  $\text{IO}_3^-$  anions whilst  $\text{I}^-$  anions stayed  
132 trapped on the resin. Total dissolved iodine concentration was measured (see 2.2.2) before the AEC ( $\text{I}^-$

133 + IO<sub>3</sub><sup>-</sup>) and in the column flow-through (IO<sub>3</sub><sup>-</sup>), I<sup>-</sup> was calculated as the difference. We checked the  
134 accuracy of the separation with the standard addition method using KI, KIO<sub>3</sub> and both together.

### 135 2.2.2 Determination of iodine concentration

136 Total dissolved iodine (as I<sup>-</sup> and/or IO<sub>3</sub><sup>-</sup>) concentration in seawater was determined by  
137 spectrophotometry according to (Sandell & Kolthoff, 1937) in the range [0.04-0.30] μM. Seawater  
138 samples were filtered (0.45 μm, Millipore ref. HAWG0700) and diluted in MilliQ water to fit within that  
139 range. The color reaction was prepared in a 1.5 mL centrifuge tube with 500 μL of either seawater or  
140 an AEC-treated seawater sample (diluted), 50 μL NaCl (10% g/g), 500 μL As<sub>2</sub>O<sub>3</sub> (0.1 M) and transferred  
141 to a water bath at 30°C. Then 125 μL of (SO<sub>4</sub>)<sub>4</sub>Ce(NH<sub>4</sub>)<sub>4</sub>, 2 H<sub>2</sub>O, (0.02 M) was added and the reaction was  
142 allowed to run for exactly 20 min at 30°C in the water bath. Absorbance at 420 nm was then measured  
143 in 1 mL disposable cuvettes in a spectrophotometer. A calibration curve was carried out with standard  
144 solutions between 0.039 μM and 0.316 μM (dilutions of 1.31 g.L<sup>-1</sup> KI in MilliQ water solution). The  
145 repeatability of the method showed that the uncertainty of the results was ± 5%. Total iodine  
146 concentration before (I<sup>-</sup> + IO<sub>3</sub><sup>-</sup>) and after (IO<sub>3</sub><sup>-</sup>) separation by AEC (see 2.2.1) was determined in order  
147 to obtain the I<sup>-</sup> concentration based on the difference. We checked the accuracy of the quantification  
148 with the standard addition method using KI, KIO<sub>3</sub> and both together. The reliability of method was  
149 further checked by comparing the results obtained by spectrophotometry with duplicates analyzed by  
150 ICPMS measurements on some of our samples.

151

### 152 2.3 Measurement of net iodine flux between seaweed and seawater

153 Plantlets of *L. digitata* (pooled to about 2 g) were incubated in beakers with 50-75 mL of filtered  
154 seawater (0.45 μm, Millipore ref. HAWG0700) at the same temperature as in the host aquarium (12.5  
155 ± 1.0 °C), with bubbling. Seawater samples were collected over time (a picture of the incubation setup  
156 is provided in the supplementary material S1-1). The sample volume was 0.5 mL for total dissolved  
157 iodine (I<sup>-</sup> + IO<sub>3</sub><sup>-</sup>) and 3 mL for AEC separation. Beakers without seaweed plantlets served as controls for  
158 changes in iodine concentrations into the filtered seawater used due to adsorption onto the beakers  
159 surface. No changes in iodine concentrations were observed in those beakers. At some point in the  
160 experiment, seawater was spiked either with KI, KIO<sub>3</sub> or both. Upon completion of each experiment,  
161 the plantlets were patted dry between absorbent paper sheets and weighed. Concentrations of both  
162 I<sup>-</sup> and IO<sub>3</sub><sup>-</sup> in the water were plotted as a function of time.

### 163 2.4 Measurement of unidirectional <sup>131</sup>I<sup>-</sup> influx in seaweed

164 Iodine-131 as KI was purchased from CIS Bio International (I-131-S-2) and the activity information  
165 was provided by the manufacturer with the calibration date (Act.=1.11E+08 Bq; Vol.=0.67 cc;  
166 <sup>131</sup>I/<sup>127</sup>I=4.64E+08). Because of constraints in accurate nuclear metrology (geometry calibration),  
167 unidirectional radioactive <sup>131</sup>I influx was measured on tissue disks punched out of *L. digitata* blade as  
168 previously published (Küpper et al, 1998; Shaw, 1959). Tissue disks were incubated in seawater spiked  
169 with <sup>131</sup>I in the form of KI. The disks were rapidly patted dry on absorbent paper, transferred to a plastic  
170 container and counted for 60 sec on a hyper pure GeHP gamma detector. The measurement procedure  
171 lasted 1.5 min and the disks were then returned to the incubation medium to carry on the uptake  
172 kinetics experiment. Radioactive iodine disk content was then plotted as a function of time and it was  
173 found to be linear for 15 min. The activity in seawater was found to be constant for short-term  
174 experiments (15 min). We investigated the relationship between the <sup>131</sup>I uptake by the disks and iodine  
175 concentration in seawater. For that purpose, seawater iodine concentration was increased by addition  
176 of KI to 1, 3, 10, 50, 500 μM and spiked with <sup>131</sup>I (230 Bq.mL<sup>-1</sup>). The slope of the 15 min linear <sup>131</sup>I uptake  
177 allowed the iodine permeability of the disks to be estimated (in nmol.min<sup>-1</sup>.g<sup>-1</sup>) since the exchange

178 surface was constant. Plotting the iodine permeability as a function of seawater concentration allowed  
179 for the derivation of the values of Vmax and Km according to the Michaelis-Menten model as  
180 previously described by (Küpper et al, 1998). The Michaelis-Menten model was fitted using Microsoft  
181 Excel™ Solver function.

182 A longer time intake experiment was carried out over 14 days with a 0.1 g plantlet kept in a 10 L  
183 tank to estimate iodine turnover by the algae. The procedure was the same as for tissue disks with the  
184 plantlet patted dry and lying in a plastic dish for gamma counting. The activity of the seawater (30  
185 Bq.mL<sup>-1</sup> seawater) was maintained constant by adding <sup>131</sup>I to compensate for intake by the plantlet as  
186 well as <sup>131</sup>I decay. The very large volume of the tank compared to the small size of the plantlet ensured  
187 that no total iodine depletion occurred in seawater. The biological half-life of iodine in *L. digitata*  
188 plantlet was estimated as  $t_{b1/2} = \ln(2)/k$  by fitting the data to equation  $Act_t = Act_0 \cdot [1 - \exp(-k \cdot t)]$  (with  
189  $t$ =time;  $Act_t$ =<sup>131</sup>I activity at time  $t$ ;  $k$ =time constant) with the Solver function of Microsoft Excel™ (we  
190 don't need to implement <sup>131</sup>I decay since the radioisotope activity is artificially maintained constant in  
191 seawater).

## 192 2.5 Measurement of iodine-129 activity in seawater

193 120 L-seawater samples were collected monthly at Goury for 37 months, and filtered at 0.45 µm  
194 (Millipore, Durapore membrane ref. HVLP2932A). Total dissolved iodine concentration was  
195 determined in an aliquot as described above (2.2.2). A known amount of stable iodine (0.500 g KIO<sub>3</sub>)  
196 was added to the 120 L as a carrier and to allow for the calculation of the extraction yield. Dissolved  
197 iodine in the forms of I<sup>-</sup> and IO<sub>3</sub><sup>-</sup> were merged by the addition of 120 g Na<sub>2</sub>SO<sub>3</sub> at pH 2 (HCl-36%) to  
198 reduce IO<sub>3</sub><sup>-</sup> into I<sup>-</sup>. Total I<sup>-</sup> was then precipitated by the addition of 6 g AgNO<sub>3</sub>. The AgI precipitate was  
199 recovered in 500 mL with MilliQ water and then solubilized by the addition of 35 g L-ascorbic acid  
200 (C<sub>6</sub>H<sub>8</sub>O<sub>6</sub>) at pH 10 (NaOH 5N). The solution containing dissolved iodine was then transferred into a  
201 separation funnel and covered with 100 mL 1,2,4-Trimethylbenzene (TMB). HNO<sub>3</sub> 65% was added until  
202 pH 2 was reached, and NaNO<sub>2</sub> added whilst pH was maintained with HNO<sub>3</sub> to oxidize iodide into I<sub>2</sub>. The  
203 funnel was vigorously shaken to trap I<sub>2</sub> in the organic phase and then left to decant. The aqueous phase  
204 was recovered and another 50 mL TMB was added to further extract I<sub>2</sub>. The two TMB organic phases  
205 were pooled (150 mL) and washed twice with 100 mL MilliQ water (the water was discarded). Extracted  
206 iodine was finally recovered from the organic phase by adding 20 mL of NaOH 0.5 N; Na<sub>2</sub>SO<sub>3</sub> 0.2 M to  
207 reduce I<sub>2</sub> into I<sup>-</sup>. The separation funnel was vigorously shaken, allowed to settle, and the 20 mL aqueous  
208 phase was recovered in a plastic vial where traces of TMB adhered to the plastic wall. The aqueous  
209 phase was finally transferred into a clean 20 cc geometry. The final 20 cc geometry contained initial +  
210 added stable iodine and unknown iodine-129. Iodine-129 activity was determined by gamma  
211 spectrometry in the 20 cc geometry previously calibrated with a standard solution (IL29-ELSF15  
212 #4793/4, provided by CEA/DAMRI), using a hyper pure GeHP gamma detector (29,78 keV double ray,  
213 emission rate 57,3%, detection limit = 0.05 Bq in the final sample with a counting time of 80 000 s, 0.03  
214 Bq in the final sample with a counting time of 240 000 s). A quenching curve was obtained by  
215 incrementing stable iodine concentration in the standard IL29-ELSF15 solution using the same 20 cc  
216 geometry: the quenching by stable iodine was lower than 15% (15% at 600 mg iodine, 5% at 200 mg  
217 iodine). Stable iodine concentration in the 20 cc geometry was determined by potentiometric method  
218 using an Orion 96-53 ionplus® Series Iodide Electrode according to the manufacturer's instructions.  
219 The iodine concentration in the geometry was used to correct the results for the extraction yield and  
220 for gamma counting quenching. Extraction yield was in the range [70%-80%]. Final results were  
221 expressed in Bq.m<sup>-3</sup> for <sup>129</sup>I and in µM for stable <sup>127</sup>I. The isotopic ratio <sup>129</sup>I/<sup>127</sup>I could then be calculated  
222 in seawater for total dissolved iodine (I<sup>-</sup> + IO<sub>3</sub><sup>-</sup>; with 1 Bq <sup>129</sup>I = 1.186E-09 mol).

## 223 2.6 Iodine-129 activity measurement in seaweed

224 In parallel with seawater, iodine-129 activity was determined in *L. digitata* and *F. serratus* samples  
 225 collected monthly (see **Erreur ! Source du renvoi introuvable.**), dried at 90°C and finely ground as  
 226 described in (Bouisset et al, 1999; Lefevre et al, 2003). In both species, stable total iodine concentration  
 227 was determined in parallel on aliquots by the CNRS/SCA (Service Central d'Analyses, Vernaison,  
 228 France). Seaweed dry material was mineralized in Schöniger combustion flasks and the solutions were  
 229 analyzed using ion exchange chromatography with electrochemical detection (the quantification limit  
 230 was 0.25 µg.L<sup>-1</sup> iodine). Final results were expressed in Bq.Kg<sup>-1</sup> dry weight for <sup>129</sup>I and in mg.Kg<sup>-1</sup> dry for  
 231 stable <sup>127</sup>I. The isotopic ratio <sup>129</sup>I/<sup>127</sup>I could then be calculated in dry seaweed material).

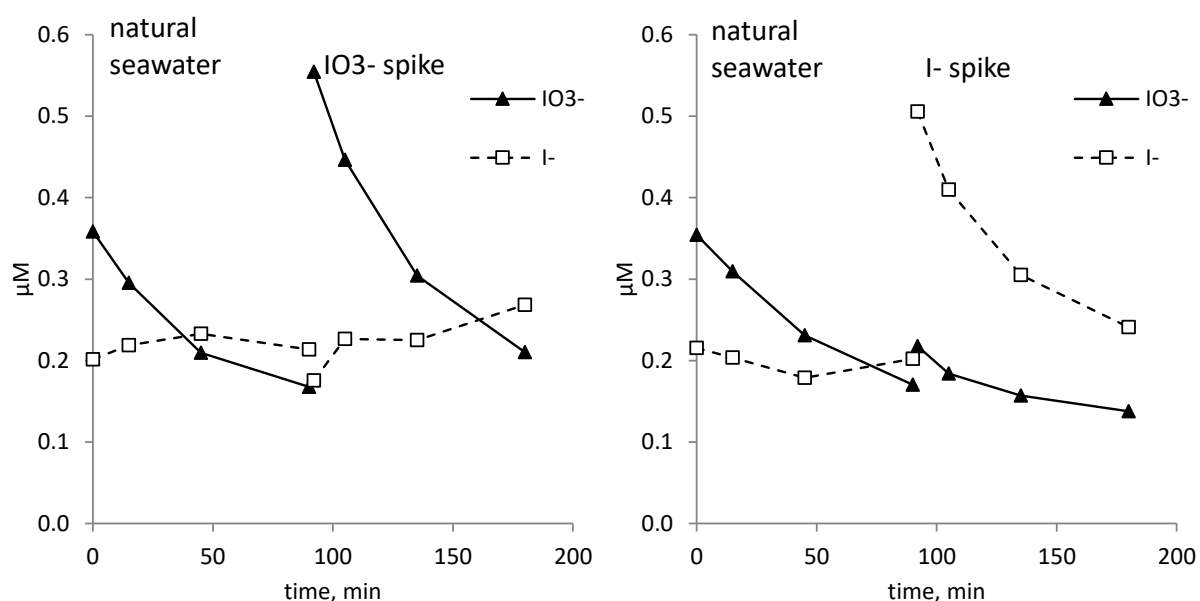
232

### 233 3 Results

#### 234 3.1 Which form of inorganic iodine in seawater is taken up by *Laminaria digitata*?

235 A first series of experiments consisted in the incubation of *L. digitata* plantlets in natural seawater  
 236 collected in Goury at the same location as the seaweed with [IO<sub>3</sub><sup>-</sup>] = 0.35 µM and [I<sup>-</sup>] = 0.25 µM. The  
 237 changes in seawater IO<sub>3</sub><sup>-</sup> and I<sup>-</sup> concentrations showed that only IO<sub>3</sub><sup>-</sup> appeared to decrease in the  
 238 medium in the presence of the plantlet, and this was confirmed by spiking seawater with IO<sub>3</sub><sup>-</sup> at time  
 239 90 min (Figure 1 left). However, spiking seawater with I<sup>-</sup> instead of IO<sub>3</sub><sup>-</sup> clearly demonstrated that both  
 240 iodine forms decreased (Figure 1 right). These experiments were replicated 6 times for I<sup>-</sup> and IO<sub>3</sub><sup>-</sup>  
 241 independently with the same results (supplementary materials S1-2 and S1-3).

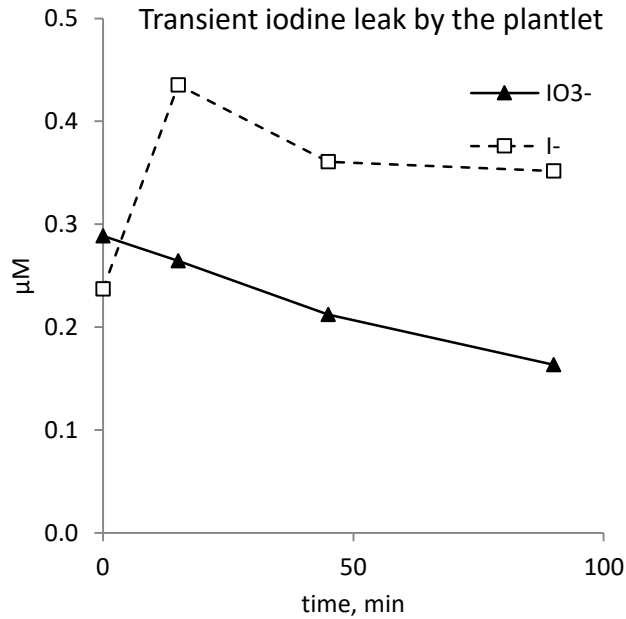
242



243

244 Figure 1: Incubation of *Laminaria digitata* plantlets: changes in seawater IO<sub>3</sub><sup>-</sup> (filled triangle) and I<sup>-</sup> (open  
 245 square) concentrations over time. The uncertainty of the measurements was ± 5 % (error bars omitted to ensure  
 246 clarity). Seawater was spiked with IO<sub>3</sub><sup>-</sup> (left) and I<sup>-</sup> (right) after 90 min of incubation.

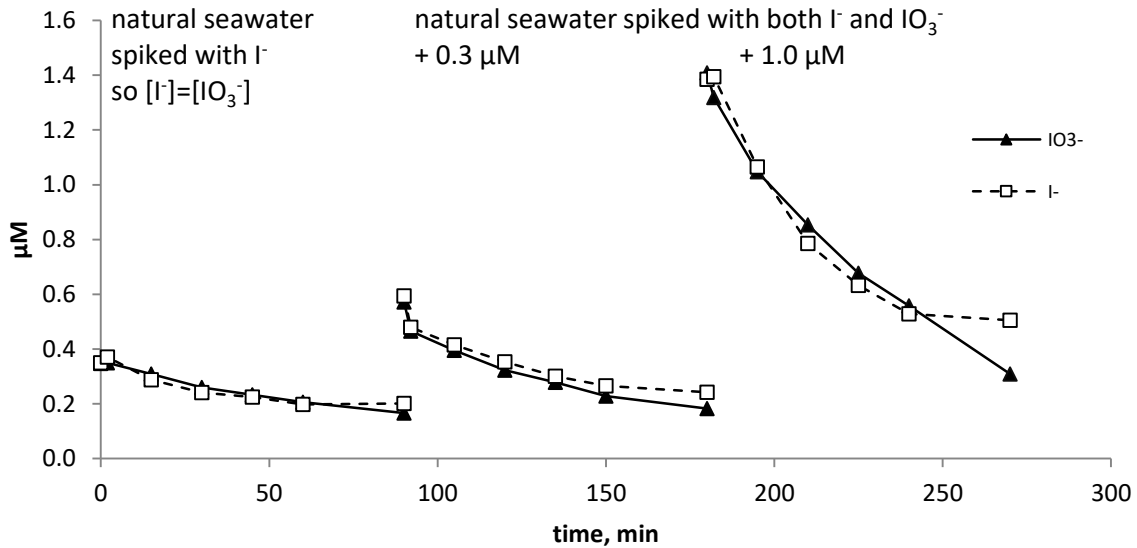
247 When replicating the experiment, the transfer of *L. digitata* plantlet to the incubation vial  
 248 sometimes resulted in transient iodine leaks from the seaweed. In those cases, only I<sup>-</sup> increased in  
 249 seawater whilst IO<sub>3</sub><sup>-</sup> continued to decline (Figure 2).



250

251 Figure 2: Transient iodine leak by the plantlet which only resulted in net  $\text{I}^-$  output whilst  $\text{IO}_3^-$  was still taken  
 252 up (same symbols as in Figure 1, uncertainties  $\pm 5\%$ ).

253 Since both  $\text{IO}_3^-$  and  $\text{I}^-$  seem to be taken up by *L. digitata*, the question then arose as to why the  $\text{I}^-$   
 254 concentration didn't decrease in the experiment illustrated in Fig.1 left? A simple hypothesis is that  
 255 the concentrations in seawater determine which form of iodine is pumped. We repeated the  
 256 experiment with different concentrations of  $\text{IO}_3^-$  and  $\text{I}^-$  in seawater, starting with the same  
 257 same concentrations of both forms of iodine, and increased the levels up to  $1.4 \mu\text{M}$  for each iodine species  
 258 (Figure 3).



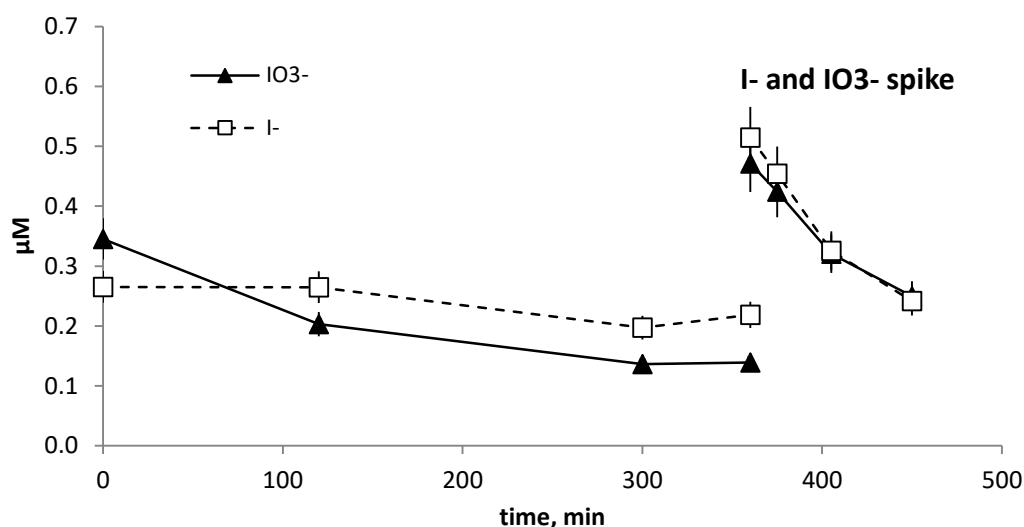
259

260 Figure 3: Incubating *Laminaria digitata* plantlets in seawater with increasing levels of  $\text{IO}_3^-$  and  $\text{I}^-$  at the same  
 261 concentration (same symbols as in Figure 1, uncertainties  $\pm 5\%$ ).

262 When both  $\text{IO}_3^-$  and  $\text{I}^-$  were present at the same concentration, their concentrations decreased  
 263 equally in the presence of the plantlet. So, in the left experiment in Figure 1, was there a minimum  $\text{I}^-$   
 264 concentration below which the uptake just balanced the output? Likewise, does a minimum  $\text{IO}_3^-$   
 265 concentration exist below which this iodine form uptake just balances the output? To address this



266 point, we extended the net flux experiment for 6 hours to attempt to see the "asymptotic" seawater  
 267  $\text{IO}_3^-$  and  $\text{I}^-$  concentrations when no more net flux were observed. At the end, the net iodine uptake was  
 268 re-stimulated by a fresh spike of  $\text{I}^-$  and  $\text{IO}_3^-$ . The results of this long-term kinetics are shown in Figure  
 269 4.

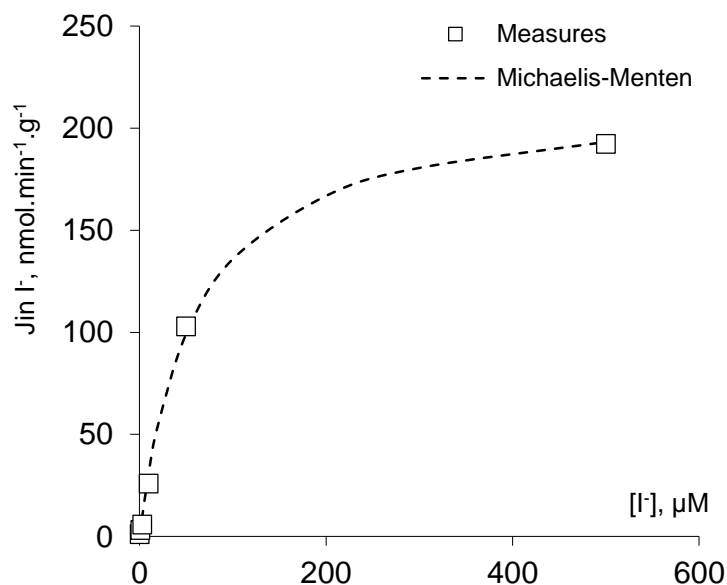


270  
 271 Figure 4: Long-term kinetics experiment on net iodine flux using plantlets of *Laminaria digitata* (same symbols  
 272 as in Figure 1).

273 This long-term kinetics experiment was replicated 7 times (supplementary materials S1-4) and  
 274 every time,  $\text{IO}_3^-$  concentrations declined below  $\text{I}^-$  concentrations, as in the example displayed in Figure  
 275 4. The average iodine concentrations ( $\pm$  SE) at time 0 were  $[\text{IO}_3^-] = 0.35 \pm 0.01 \mu\text{M}$ ;  $[\text{I}^-] = 0.31 \pm 0.06 \mu\text{M}$   
 276 and at time 360 min, they were  $[\text{IO}_3^-] = 0.16 \pm 0.03 \mu\text{M}$ ;  $[\text{I}^-] = 0.29 \pm 0.03 \mu\text{M}$ , (N=7).

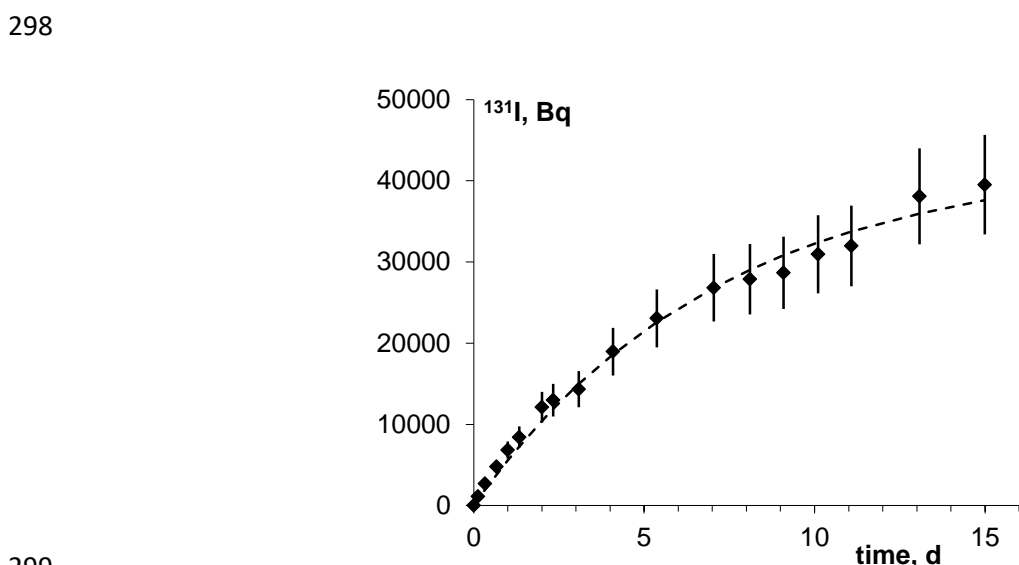
### 277 3.2 Tracing iodine uptake in *Laminaria digitata* with $^{131}\text{I}$

278 Since both  $\text{IO}_3^-$  and  $\text{I}^-$  seemed to be taken up equally by the seaweed (provided their concentrations  
 279 were high enough), using radioactive  $^{131}\text{I}^-$  was considered to trace dissolved iodine uptake whatever  
 280 the chemical form. We investigated the relationship between the uptake and iodine concentration for  
 281 *L. digitata* using disks punched out from the thallus blade as previously described (Küpper et al, 1998;  
 282 Shaw, 1959). The unidirectional flux  $J_{in}$  ( $\text{nmol}\cdot\text{min}^{-1}\cdot\text{g}^{-1}$ ) was proportional to seaweed iodine  
 283 permeability, since the disk surface was constant during the experiment. The results are presented in  
 284 Figure 5 fitted with Michaelis-Menten model kinetics with apparent  $K_m = 59 \mu\text{M}$  and  $V_{max} = 216$   
 285  $\text{nmol}\cdot\text{min}^{-1}\cdot\text{g}^{-1}$ . From those results, we calculate an approximate unidirectional influx capacity of  $^{131}\text{I}$  of  
 286 c.a.  $100 \text{ nmol}\cdot\text{min}^{-1}\cdot\text{g}^{-1}$ . This unidirectional influx can be compared to results obtained in our net fluxes  
 287 experiments (Figures 1 to 4), in which we obtained influxes of around  $1 \text{ nmol}\cdot\text{min}^{-1}\cdot\text{g}^{-1}$ . Net fluxes result  
 288 from the balance between input and output fluxes. Therefore, the 2 orders of magnitude higher  
 289 unidirectional input fluxes measured in our  $^{131}\text{I}$  uptake experiment indicate that output fluxes must be  
 290 very high to result in a 100 fold reduction when considering net fluxes.



291  
 292 Figure 5: Relationship between unidirectional iodine influx and seawater iodine concentration for tissue disks  
 293 of *Laminaria digitata*. Fitting the Michaelis-Menten model kinetics yielded  $K_m = 59 \mu\text{M}$  and  $V_{\text{max}} = 216$   
 294  $\text{nmol}\cdot\text{min}^{-1}\cdot\text{g}^{-1}$ .

295 A two-week experiment was performed to estimate the biological half-life of iodine in *L. digitata*  
 296 plantlets. The <sup>131</sup>I uptake experiment displayed in Figure 6 yielded an estimated  $t_{b1/2}$  value of c.a. 5  
 297 days.



299  
 300 Figure 6: <sup>131</sup>I uptake over two weeks by *Laminaria digitata* plantlet leading to the estimation of the iodine  
 301 turnover in the seaweed as 5 days.

302 3.3 <sup>129</sup>I transfer between seawater and brown seaweed exposed to discharges from the  
 303 ORANO reprocessing plant in La Hague

304 3.3.1 Seasonal changes of iodine in seawater and in brown seaweed

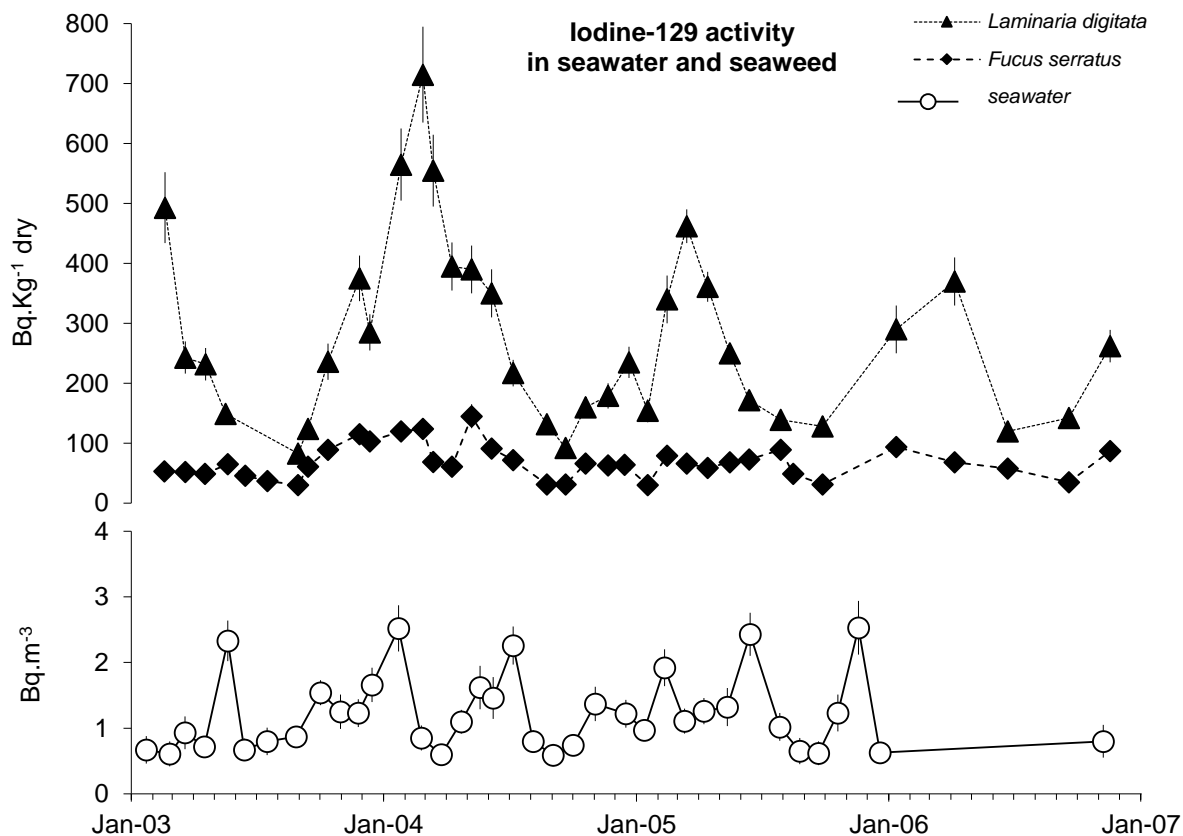
305 Seawater samples were periodically collected in Goury and analyzed for iodine chemical speciation.  
 306 Additional samples were collected in different locations around the Cap of La Hague and along the  
 307 coast of Brittany (Bretagne, France). The data are presented in the supplementary material (S2-2).

308 Since brown seaweed iodine content may vary during the seasonal cycle, it was crucial to take these  
 309 changes into account when looking at radioactive iodine transfer to seaweed. Total iodine in  $\text{mg.Kg}^{-1}$   
 310 dry was determined in *L. digitata* and *F. serratus* samples were collected monthly in Goury. The data  
 311 are displayed in the supplementary material (S2-3).

312 3.3.2 Iodine-129 activity in seawater and in brown seaweed

313 Iodine-129 activity determined in dissolved iodine in seawater ( $\text{IO}_3^- + \text{I}^-$ ) and in the two brown  
 314 seaweed species *L. digitata* and *F. serratus* are presented in Figure 7.

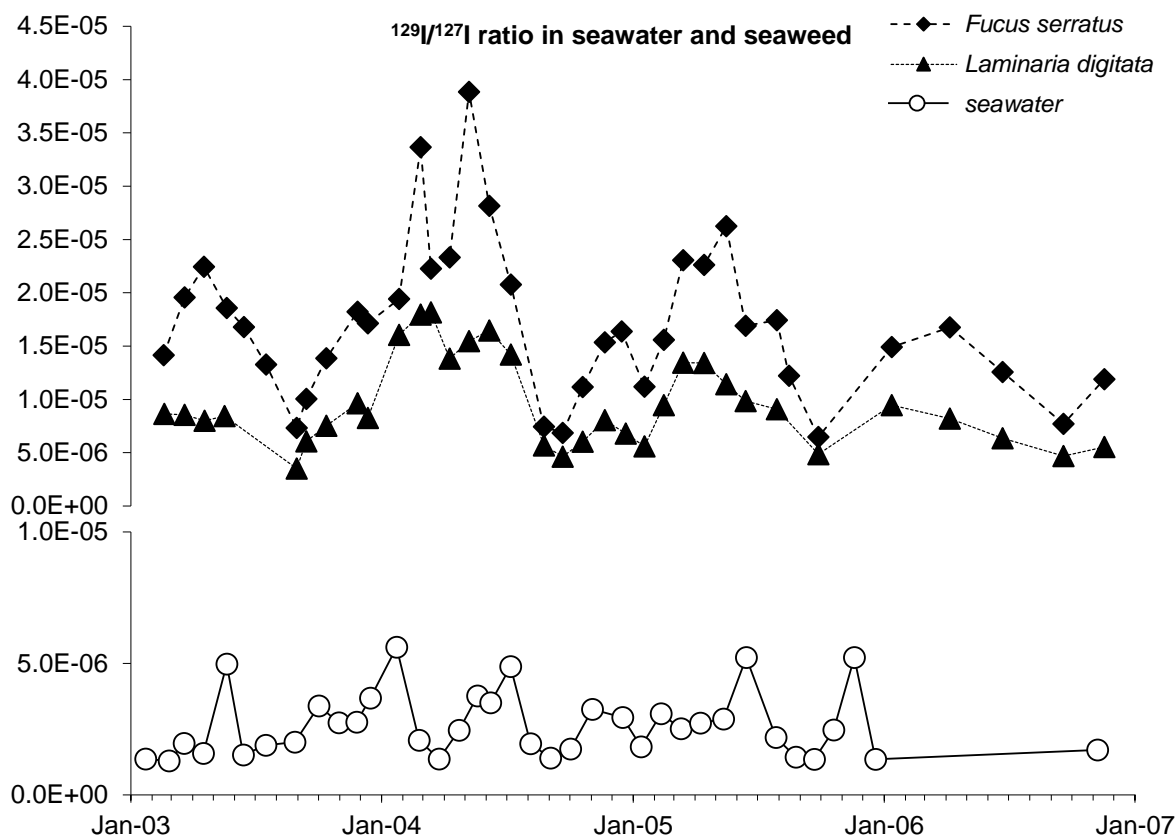
315



316

317 Figure 7: Iodine-129 activity in seawater and in brown seaweed collected in Goury, near the outlet of the  
 318 ORANO reprocessing plant in La Hague. Error bars account for metrological uncertainties (2 x sigma; may be  
 319 masked by symbol).

320 Because iodine content varies in seaweed over the season, expressing the radioactivity data as the  
 321 isotopic ratio  $^{129}\text{I}/^{127}\text{I}$  was necessary to explore  $^{129}\text{I}$  transfer between seawater and seaweed. The ratio  
 322  $^{129}\text{I}/^{127}\text{I}$  was determined in dissolved iodine in seawater ( $\text{I}^- + \text{IO}_3^-$ ) and in *L. digitata* and *F. serratus* dry  
 323 material and the data are presented in Figure 8.



324

325 Figure 8: Iodine-129 isotopic ratio in seawater and in brown seaweed collected in Goury, near the outlet of  
 326 the ORANO reprocessing plant in La Hague.

327 **4 Discussion**

328 The fate of  $^{129}\text{I}$  liquid discharged by the ORANO reprocessing plant in La Hague (Normandy, France)  
 329 deserves special attention for several reasons: due to its very slow decay, this radionuclide is a major  
 330 residual iodine radioisotope in the nuclear fuel cycle and a tracer of the discharges by the ORANO  
 331 reprocessing plant in the environment. As part of the liquid waste released in seawater in the Alderney  
 332 Race (Baillly du Bois et al, 2020; Fiévet et al, 2020), it mixes with natural stable iodine so that isotopic  
 333 dilution minimizes its impact in terms of radioprotection. However, brown seaweed is known to be  
 334 exceptionally efficient at bioaccumulating iodine from seawater. The recommended value for the  
 335 iodine concentration factor (CF) in macroalgae is  $10^4$  (IAEA, 2004), and ratios of up to  $4.3 \cdot 10^4$  were  
 336 observed in kelps (Fiévet et al, 2021). Moreover, brown seaweed has the ability to transform  
 337 accumulated iodine into volatile compounds, such as  $\text{I}_2$ , released in response to various stresses, such  
 338 as emersion at low tide (Ball et al, 2010; McFiggans et al, 2010; McFiggans et al, 2004; O'Dowd et al,  
 339 2002; Whitehead et al, 2009). This process might challenge the strategy to keep  $^{129}\text{I}$  away from humans  
 340 because the isotope can return to the terrestrial environment *via* airborne routes *via* the wind and  
 341 aerosols. For these reasons, although the potential contribution of this atmospheric route is not  
 342 known, brown seaweed is focused on as part of radionuclide monitoring of the marine environment.  
 343 Understanding the transfer of radioactive iodine released by the nuclear industry (under control) in  
 344 the marine environment is not only essential for the sake of radioprotection, the fate of radioactive  
 345 iodine released into the English Channel also has a much larger scope than radioprotection as a  
 346 potential tracer of the complex behavior of iodine in the marine environment. The different key steps  
 347 of iodine transfer from seawater to the bioaccumulation in brown seaweed are part of the bigger  
 348 puzzle of the biogeochemical cycle of iodine in the ocean and its consequences on the chemistry of  
 349 the atmosphere (Carpenter et al, 2021). The transfer of iodine from the ocean to the atmosphere is

350 assumed to occur through the oxidation of iodide ( $I^-$ ) into diiodine ( $I_2$ ) in the presence of atmospheric  
351 ozone under solar radiation, but also through biological oxidation processes (Carpenter et al, 2021).  
352 Iodate ( $IO_3^-$ ) is the preferential chemical form of iodine in seawater, therefore its conversion into iodide  
353 ( $I^-$ ) is not spontaneous as regards thermodynamics (Hou et al, 2007; Wong, 1991). After decades of  
354 literature on the topic, the reduction of iodate into iodide still remains poorly understood, though  
355 microorganisms or marine algae clearly play a role (Carpenter et al, 2021; Wong, 1991) and this factor  
356 has recently been confirmed for some marine bacteria (Reyes-Umana et al, 2022).

357 In the present study, we provide new information on the uptake mechanism of iodine by kelp (*L.*  
358 *digitata*). First, our results suggest that kelp plantlets were able to take up iodine in the forms of both  
359  $IO_3^-$  and  $I^-$  with the same efficiency (Figure 1). When both iodine species were present at the same  
360 concentration, they declined at equivalent rates in seawater (Figure 3). It should be emphasized that  
361 our experimental conditions magnified naturally occurring phenomena due to a change in the ratio  
362 between the seaweed mass and the volume of its surrounding seawater compared to the natural  
363 environment. This magnification allowed us to easily assess the net  $IO_3^-$  and  $I^-$  fluxes between the  
364 plantlet and seawater by measuring the decrease in those iodine species in seawater, with our  
365 measurements accounting for the balance between inputs and outputs. Plantlets of *L. digitata* are very  
366 sensitive and required extreme care during transfers from the natural environment and between the  
367 host aquarium and the flux experiment setup. Chemical imaging data provided information on a very  
368 unequal compartmentalization of iodine in the tissue of *L. digitata* plantlet. Iodine appears to be  
369 preferentially concentrated in the peripheral apoplastic tissue (Lebeau et al, 2021). As such, transient  
370 iodine leakage might occur when manipulating a plantlet. We assumed that plantlets underwent  
371 minimal stress because after each experiment, they were returned to the host aquarium and could be  
372 re-used for more experiments, and the iodine leaks sometimes observed at the beginning of the  
373 experiments were only transient and brief. Indeed, a transient iodine leak by the plantlets was  
374 observed in 11 out of 42 net flux experiments. In all cases it should be emphasized that only  $I^-$  leaks  
375 were ever detected in seawater whilst  $IO_3^-$  always continued to decline (Figure 2). This observation was  
376 an *in vivo* evidence that iodine is stored in *L. digitata* tissue as iodide ( $I^-$ ), as shown by laser  
377 desorption/ionization mass spectrometry (Lebeau et al, 2021). We could then interpret the results of  
378 our net flux experiment on the basis of this information. When assessing  $IO_3^-$  and  $I^-$  net fluxes, we  
379 expected those fluxes to stop when the inputs balanced the outputs, or when the seawater  
380 concentrations were too low to meet the needs of the uptake process. In the long-term (6 hours)  
381 experiment (Figure 4), a change in seawater iodine speciation was observed in the presence of *L.*  
382 *digitata* plantlets. The  $IO_3^-$  concentration was initially above the  $I^-$  concentration, and this reversed  
383 after 2 hours.  $IO_3^-$  declined down to around 0.15  $\mu M$  whilst  $I^-$  stayed at around 0.25  $\mu M$ . If the seaweed  
384 only stores  $I^-$  but can take up both  $IO_3^-$  and  $I^-$ , we conclude that  $IO_3^-$  was likely to be converted into  $I^-$  at  
385 some point in the plantlet (apoplast), or through the action of associated microorganisms. After 5-6  
386 hours of incubation, the stable  $IO_3^-$  and  $I^-$  concentrations in seawater therefore resulted from  $IO_3^- + I^-$   
387 influxes and  $I^-$  outflux only. We assume that the  $IO_3^-$  stabilized in seawater because its concentration  
388 was so low that the uptake mechanism was no longer able to pump this iodine form, "by exhaustion",  
389 as indicated by the more than 200 fold difference between the  $K_M$  of 59  $\mu M$  and the final iodine  
390 concentrations of 0.15-0.25  $\mu M$  we measured. Conversely, the extreme chemical gradient of  $I^-$   
391 between the seaweed and seawater and its permeability resulted in  $I^-$  outflux.  $I^-$  stabilization in  
392 seawater corresponded to the balance between this  $I^-$  leak and the ability of the mechanism to take  
393 up  $I^-$ . So, when the  $IO_3^-$  is low enough in seawater to exhaust its uptake, we only observe  $I^-$  recycling. A  
394 major conclusion of this laboratory experiment was that we directly observed the kelp-based biogenic  
395 conversion of seawater  $IO_3^-$  into  $I^-$ . Even if the quantitative contribution of the process was considerably

396 magnified with our biomass/seawater ratio, this provided direct evidence of this iodine conversion  
397 mediated by brown algae and associated microorganisms observed in the marine environment.

398 Second, we also concluded that *L. digitata* plantlets can take up either  $\text{IO}_3^-$  or  $\text{I}^-$  indifferently. Iodine  
399 bioaccumulation in kelps is assumed to be mediated by vanadium-dependent haloperoxidases (VHPO)  
400 family (Küpper et al, 1998), and especially by vanadium-dependent iodoperoxidases (VIPO)  
401 characterized in *L. digitata*, specific to iodide oxidation (Colin et al, 2005). The substrates of VHPOs are  
402 halides and  $\text{H}_2\text{O}_2$  (Colpas et al, 1996) so VIPO is assumed to oxidize  $\text{I}^-$  and not  $\text{IO}_3^-$ . The hypothetical  
403 mechanism involving only VIPO-based iodide uptake in iodine bioaccumulation by kelp was recently  
404 questioned by our data on the apoplastic localization of iodine storage in the plantlets (Lebeau et al,  
405 2021; Verhaeghe et al, 2008). The parallel uptake of  $\text{IO}_3^-$  and  $\text{I}^-$  that we observed in our net flux  
406 experiments suggests a need to further validate *in vivo* the biological function of VHPO and/or VIPO in  
407 iodine bioaccumulation. However, we suggest the following speculative scheme: if iodide is the only  
408 form of iodine in the storage site, as shown previously (Lebeau et al, 2021; Verhaeghe et al, 2008),  
409 oxidized forms may have a favorable chemical gradient to enter the seaweed. This would rely on the  
410 strong reduction capacity of the storage site in order to maintain this gradient. The question of this  
411 reduction capacity inside the seaweed storage compartment is still pending, but in this scheme, the  
412 driving force would be this reduction capacity of the apoplastic storage site and the uptake would only  
413 rely on oxidized iodine accessing the site along a favorable chemical gradient. Natural  $\text{IO}_3^-$  in seawater  
414 would be available for this, and VIPO would be there to oxidize  $\text{I}^-$  when present. It should be kept in  
415 mind that a major role for the  $\text{I}^-$  bioaccumulated in the seaweed is to react with reactive oxygen species  
416 to reduce oxidative stress and/or to release oxidized iodine in response to stress as a defense  
417 mechanism (Küpper et al, 2008).

418 We used an  $^{131}\text{I}$  tracer to further characterize iodine uptake in kelp. This replicated a kinetic  
419 experiment (3 hours) performed many decades ago (Shaw, 1959). The isotope was added in the form  
420 of  $^{131}\text{I}^-$ , but our net flux experiment showed that both  $\text{IO}_3^-$  and  $\text{I}^-$  uptakes exactly matched. This  
421 suggested that  $^{131}\text{I}^-$  unidirectional influx data were relevant to trace iodine uptake. The dependence of  
422  $\text{I}^-$  uptake on concentration followed Michaelis-Menten kinetics, as previously published with disks of  
423 *L. digitata* (Küpper et al, 1998). The Michaelis-Menten kinetics confirmed the enzymatic mediation of  
424  $\text{I}^-$  uptake but our values of  $K_m$  and  $V_m$  parameters were quite different. Our  $K_m$  value of  $59\ \mu\text{M}$  was  
425 more than 7 times lower and our  $V_m$  value of  $219\ \mu\text{M}$  was more than three times higher. We have no  
426 explanation for this discrepancy except maybe the physiological condition of the disks punched out  
427 from the blade of *L. digitata*. On the basis of our  $K_m$  value of  $59\ \mu\text{M}$ , we may speculate that at  
428 concentrations more than two orders of magnitude lower, like in our flux experiments (Figure 4), the  
429 uptake mechanism reached a steady state. A biological half-life of 5 days for iodine was estimated  
430 based on the long-term  $^{131}\text{I}^-$  uptake experiment on *L. digitata* plantlets. Although the values are  
431 consistent, this was below our previous estimate of 14 days in brown seaweed based on modeling  
432 using  $^{129}\text{I}$  environmental data (*L. digitata* and *F. serratus*) in the marine environment in the vicinity of  
433 the ORANO reprocessing plant in La Hague (Fiévet et al, 2021). Our laboratory experiment lasted 15  
434 days, but we can't rule out that we had not reached the plateau for  $^{131}\text{I}$  activity in the seaweed. Besides,  
435 it was not surprising that the young plantlet of *L. digitata* showed small differences in iodine uptake  
436 kinetics compared to adult and other brown seaweed used in our environmental modelling.

437 The apparent convergence of  $\text{IO}_3^-$  and  $\text{I}^-$  uptake by *L. digitata* plantlets observed in our net flux  
438 experiments was essential for interpreting our study of radioactive iodine transfer between seawater  
439 and seaweed in the marine environment under the influence of radioactive liquid discharges from the  
440 ORANO reprocessing plant in La Hague.  $^{129}\text{I}$  should be measured in seawater based on total iodine ( $\text{IO}_3^-$   
441 +  $\text{I}^-$ ) to account for  $^{129}\text{I}$  bioavailability at least for kelps. Seasonal changes in iodine concentrations in

442 seawater and in seaweed were also essential to take into account. In seawater, if we merge all total  
443 ( $\text{IO}_3^- + \text{I}^-$ ) dissolved iodine measurements we took in seawater along the coast of the English Channel  
444 and Brittany (Map in the supplementary material S2-1), the average concentration ( $\pm$  SE) was  $0.54 \pm$   
445  $0.05 \mu\text{M}$  ( $N=56$ ). Our recent measurements around the Cape of La Hague (supplementary material S2-  
446 2) with  $\text{IO}_3^-$  and  $\text{I}^-$  partitioning showed relatively stable  $\text{IO}_3^-$  concentration whilst  $\text{I}^-$  seemed to fluctuate  
447 over the year. Longer time-series measurements are required to confirm these chemical speciation  
448 data, but a question already arose from these  $\text{I}^-$  data. In seawater samples collected from the shore,  
449 where brown seaweed including kelp was present, our  $\text{IO}_3^-$  concentration measurements of around  
450  $0.3 \mu\text{M}$  were consistent with offshore values reported in the literature (Hou et al, 2007). But our  $\text{I}^-$   
451 concentrations onshore were around  $0.2 \mu\text{M}$ , whilst they were in the range  $[0.04-0.08] \mu\text{M}$  in the  
452 middle of the English Channel. Interestingly, iodide concentrations around  $0.15 \mu\text{M}$  were reported at  
453 coastal sampling locations from North Germany (Hou et al, 2007). This difference in iodide partition  
454 between coastal and offshore waters is in agreement with previous reviews by (Wong, 1991; Wong,  
455 2001; Wong & Cheng, 2001a; Wong & Cheng, 2001b). Did the presence of local brown algae fields  
456 influence the iodine chemical partition ( $\text{IO}_3^-$  vs  $\text{I}^-$ ) in our coastal seawater sample? This question is now  
457 under further investigation (Carrano et al, 2021). Nevertheless, total dissolved iodine concentration  
458 data in seawater were used to calculate the isotopic ratio of  $^{129}\text{I}$  in total iodine ( $\text{IO}_3^- + \text{I}^-$ ) measurements  
459 in Goury (Figure 7 and Figure 8). Iodine content in brown seaweed clearly cycled with season, with  
460 higher levels in winter than in summer (supplementary material S2-3). Does a higher growth rate in  
461 summer overwhelm the iodine uptake capacity of the seaweed? Does solar exposure at low tide or  
462 other stresses (thallus grazing by marine organisms) result in more volatile iodine release and loss?  
463 Regardless of the cause, it was critical to consider iodine seasonal fluctuations in seaweed (Ar Gall et  
464 al, 2004) when investigating radioactive iodine transfer between seawater and seaweed. The isotopic  
465 ratio  $^{129}\text{I}/^{127}\text{I}$  in seaweeds and in seawater gave us a better understanding of iodine transfer. Up to 10-  
466 fold higher isotopic ratios were found in seaweed vs seawater (Figure 8). Although the  $^{129}\text{I}$  activities  
467 were lower in *F. serratus* than in *L. digitata* (Figure 7), the  $^{129}\text{I}/^{127}\text{I}$  ratio values in the former were above  
468 those in the latter (Figure 8). The discrepancy between the isotopic ratio  $^{129}\text{I}/^{127}\text{I}$  in seawater and brown  
469 seaweed was puzzling. Our net laboratory  $\text{IO}_3^-$  and  $\text{I}^-$  flux experiments in *L. digitata* plantlets showed  
470 that both forms of iodine are equally taken up by the seaweed. Therefore, a conversion of  $^{129}\text{I}^-$   
471 discharged by the reprocessing plant into  $^{129}\text{IO}_3^-$  would not result in a change in  $^{129}\text{I}^-$  bioavailability for  
472 kelp, as we had however proposed in our recent review (Fiévet et al, 2021). This also invalidates this  
473 hypothesis to explain why the apparent  $^{129}\text{I}^-$  bioavailability declined with distance from the plant outlet,  
474 as we noticed in seaweed with regards to hydrodynamic dispersion modelling (Fiévet et al, 2021). We  
475 cannot currently explain the difference in the isotopic ratio  $^{129}\text{I}/^{127}\text{I}$  between seawater and brown  
476 seaweed. Although we cannot rule out isotopic fractionation in the uptake mechanism, it seems  
477 unlikely with such a small relative difference in the nucleus mass of the two iodine isotopes. A likely  
478 explanation was that, when looking at  $\text{IO}_3^- + \text{I}^-$  in seawater, we missed an essential  $^{129}\text{I}$  compartment  
479 (chemical form) in the marine environment to which brown seaweed are exposed, an iodine  
480 compartment that remains to be identified. The difference in the isotopic ratio  $^{129}\text{I}/^{127}\text{I}$  between the  
481 two seaweed species that we analyzed may provide a clue. *F. serratus* grows in the mid intertidal zone  
482 whilst *L. digitata* grows at the very bottom. It means that the former emerges twice a day at low tide  
483 and the latter only a few times a month during spring tides. More frequent contact with the seawater  
484 surface and longer contact with the atmosphere occurs for *Fucus* than *Laminaria*. To test this  
485 hypothesis in a preliminary experimental setup, we detached adult *L. digitata* from the rocks and  
486 artificially maintained the seaweed in a floating net for 1 month (photo in the supplementary material  
487 S2-4). At the same location, we compared  $^{129}\text{I}$  activities in natural specimens from the bottom with  
488 those from the net and observed a 50% increase (not shown). The thallus tissue was not visibly  
489 degraded, and an identical  $^{40}\text{K}$  level was taken as an indication of regular mineral balance. This

490 experiment was anecdotal and should be confirmed and further characterized. The question raised by  
491 the different isotopic ratio  $^{129}\text{I}/^{127}\text{I}$  between seawater and brown seaweed is still open, but the sea  
492 surface and its interface with the atmosphere may be a focal point when investigating iodine transfer  
493 to seaweed in the marine environment.

## 494 **5 Conclusion**

495 The present paper aimed to improve our understanding of iodine transfers between seawater and  
496 brown seaweed in the context of radioactive liquid discharges from nuclear facilities in the marine  
497 environment. We are left with a series of questions: 1- The iodine uptake mechanism in brown  
498 seaweed, which yields an exceptional bioaccumulation level, unknown in any other living organism, is  
499 still mysterious. The difference of five orders of magnitude in concentration with respect to seawater  
500 is even a low estimate, since iodine storage compartments are probably only peripheral in the  
501 apoplast, as suggested by previous results in *L. digitata* (Lebeau et al, 2021; Verhaeghe et al, 2008).  
502 However, our net  $\text{IO}_3^-$  and  $\text{I}^-$  flux experiments demonstrated that both iodine chemical forms are taken  
503 up by *L. digitata* plantlets. The role of iodoperoxidases identified in this species and hypothesized to  
504 be key to specific iodide uptake (Colin et al, 2005) remains to be further validated *in vivo*. In this new  
505 context, a reduction process is likely to be a key step for completing the picture. 2- No step in the  
506 radioactive iodine biological cycle between seawater and brown seaweed is expected to change the  
507 isotopic ratio, except unlikely isotopic fractionation. However, our environmental data on the isotopic  
508 ratio  $^{129}\text{I}/^{127}\text{I}$  in seawater and brown seaweed exposed to liquid discharges from the ORANO  
509 reprocessing plant in La Hague showed an unexpected discrepancy. This means that this *in situ*  
510 monitoring certainly missed a key compartment involved in  $^{129}\text{I}$  transfer between seawater and brown  
511 seaweed. The question raised in our previous review on radioactive transfers in the marine  
512 environment around the reprocessing plant (Fiévet et al, 2021) regarding the non-conservative  
513 hydrodynamic dispersion of  $^{129}\text{I}$  also remains open. Although important questions remain to be  
514 addressed, our laboratory experiments provided a direct observation of the ability of marine brown  
515 algae to modify iodine chemical speciation in seawater and to convert seawater  $\text{IO}_3^-$  into  $\text{I}^-$ . The  
516 endogenous extracellular pathways through which seaweed modify iodine chemistry in seawater  
517 remain to be further investigated. This conversion is a key step in the Earth's biogeochemical iodine  
518 cycle between the Ocean and the Atmosphere (Carpenter et al, 2021).

## 519 **6 Acknowledgment**

520 The authors are indebted to Frédéric COPPIN, Loïc CARASCO, Sarah ZAMANE from the Laboratoire  
521 de recherche sur les transferts des radionucléides au sein des écosystèmes terrestres (IRSN/PSE-  
522 ENV/SRTE) for ICPMS measurements on some of our samples to confirm the reliability of the  
523 spectrophotometry method used to determine iodine concentration.

## 524 **7 Funding**

525 This work benefited from the support of the Centre National de la Recherche Scientifique (CNRS)  
526 and the Institut de Radioprotection and Sureté Nucléaire (IRSN). This collaborative project (KELPS and  
527 MARIO) was funded by the NEEDS Environnement program (CNRS-IRSN-CEA).

528

## 529 **8 Supplementary material**

530 Additional data are provided in two files: Supplementary\_Material\_1.pdf and  
531 Supplementary\_Material\_2.pdf.



532 **9 References**

533 Ar Gall E, Küpper FC, Kloareg B (2004) A survey of iodine content in *Laminaria digitata*. *Botanica Marina*  
534 **47**: 30-37

535  
536 Bailly du Bois P, Dumas F, Morillon M, Furgerot L, Voiseux C, Poizot E, Méar Y, Bennis AC (2020) The  
537 Alderney Race: general hydrodynamic and particular features. *Philosophical transactions Series A,*  
538 *Mathematical, physical, and engineering sciences* **378**: 20190492

539  
540 Ball SM, Hollingsworth AM, Humbles J, Leblanc C, Potina P, McFiggans G (2010) Spectroscopic studies  
541 of molecular iodine emitted into the gas phase by seaweed. *Atmospheric Chemistry and Physics* **10**:  
542 6237-6254

543  
544 Bouisset P, Lefevre O, Cagnat X, Kerlau G, Ugron A, Calmet D (1999) Direct gamma-X spectrometry  
545 measurement of <sup>129</sup>I in environmental samples using experimental self-absorption corrections.  
546 *Nuclear Instruments and Methods in Physics Research Section A: Accelerators, Spectrometers,*  
547 *Detectors and Associated Equipment* **437**: 114-127

548  
549 Carpenter LJ (2003) Iodine in the marine boundary layer. *Chemical Reviews* **103** 4953-4962

550  
551 Carpenter LJ, Chance RJ, Sherwen T, Adams TJ, Ball SM, Evans MJ, Hepach H, Hollis LDJ, Hughes C,  
552 Jickells TD, Mahajan A, Stevens DP, Tinel L, Wadley MR (2021) Marine iodine emissions in a changing  
553 world. *Proceedings of the Royal Society A: Mathematical, Physical and Engineering Sciences* **477**:  
554 20200824

555  
556 Carpenter LJ, MacDonald SM, Shaw MD, Kumar R, Saunders RW, Parthipan R, Wilson J, Plane JMC  
557 (2013) Atmospheric iodine levels influenced by sea surface emissions of inorganic iodine. *Nature*  
558 *Geoscience* **6**: 108-111

559  
560 Carrano MW, Carrano CJ, Edwards MS, Al-Adilah H, Fontana Y, Sayer MDJ, Katsaros C, Raab A,  
561 Feldmann J, Küpper FC (2021) *Laminaria* kelps impact iodine speciation chemistry in coastal seawater.  
562 *Estuarine, Coastal and Shelf Science* **262**: 107531

563  
564 Chance R, Baker AR, Carpenter L, Jickells TD (2014) The distribution of iodide at the sea surface.  
565 *Environmental Sciences: Processes and Impacts* **16**: 1841-1859

566  
567 Colin C, Leblanc C, Michel G, Wagner E, Leize-Wagner E, Van Dorsselaer A, Potin P (2005) Vanadium-  
568 dependent iodoperoxidases in *Laminaria digitata*, a novel biochemical function diverging from brown  
569 algal bromoperoxidases. *Journal of Biological Inorganic Chemistry* **10**: 156-166

570  
571 Colpas GJ, Hamstra BJ, Kampf JW, Pecoraro VL (1996) Functional Models for Vanadium  
572 Haloperoxidase: Reactivity and Mechanism of Halide Oxidation. *Journal of the American Chemical*  
573 *Society* **118**: 3469-3478

574

575 Fiévet B, Bailly du Bois P, Voiseux C (2021) Concentration factors and biological half-lives for the  
576 dynamic modelling of radionuclide transfers to marine biota in the English Channel. *Science of The*  
577 *Total Environment* **791**: 148193

578

579 Fiévet B, Bailly du Bois P, Voiseux C, Godinot C, Cazimajou O, Solier L, De Vismes Ott A, Cossonnet C,  
580 Habibi A, Fleury S (2020) A comprehensive assessment of two-decade radioactivity monitoring around  
581 the Channel Islands. *Journal of Environmental Radioactivity* **223-224**: 106381

582

583 Fuge R, Johnson CC (2015) Iodine and human health, the role of environmental geochemistry and diet,  
584 a review. *Applied Geochemistry* **63**: 282-302

585

586 Hou X, Aldahan A, Nielsen SP, Possnert G, Nies H, Hedfors J (2007) Speciation of <sup>129</sup>I and <sup>127</sup>I in seawater  
587 and implications for sources and transport pathways in the North Sea. *Environmental Science &*  
588 *Technology* **41**: 5993-5999

589

590 Hou X, Dahlgard H, Nielsen SP (2001) Chemical speciation analysis of <sup>129</sup>I in seawater and a  
591 preliminary investigation to use it as a tracer for geochemical cycle study of stable iodine. *Marine*  
592 *Chemistry* **74**: 145-155

593

594 IAEA. (2004) Sediment distribution coefficients and concentration factors for biota in the marine  
595 environment. International Atomic Energy Agency, Vienna, p. 103.

596

597 Kolb C (2002) Iodine's air of importance. *Nature* **214**: 597-598

598

599 Küpper F, Schweigert N, Ar Gall E, Legendre J, Vilter H, Kloareg B (1998) Iodine uptake in Laminariales  
600 involves extracellular haloperoxidase-mediated oxidation of iodide. *Planta* **207**: 163-171

601

602 Küpper FC, Carpenter LJ, McFiggans GB, Palmer CJ, Waite TJ, Boneberg EM, Woitsch S, Weiller M, Abela  
603 R, Grolimund D, Potin P, Butler A, Luther lii GW, Kroneck PMH, Meyer-Klaucke W, Feiters MC (2008)  
604 Iodide accumulation provides kelp with an inorganic antioxidant impacting atmospheric chemistry.  
605 *Proceedings of the National Academy of Sciences of the United States of America* **105**: 6954-6958

606

607 Lebeau D, Leroy N, Doizi D, Wu T-D, Guerquin-Kern J-L, Perrin L, Ortega R, Voiseux C, Fournier J-B, Potin  
608 P, Fiévet B, Leblanc C (2021) Mass spectrometry – based imaging techniques for iodine-127 and iodine-  
609 129 detection and localization in the brown alga *Laminaria digitata*. *Journal of Environmental*  
610 *Radioactivity* **231**: 106552

611

612 Leblanc C, Colin C, Cosse A, Delage L, La Barre S, Morin P, Fiévet B, Voiseux C, Ambroise Y, Verhaeghe  
613 E, Amouroux D, Donard O, Tessier E, Potin P (2006) Iodine transfers in the coastal marine environment:  
614 the key role of brown algae and of their vanadium-dependent haloperoxidases. *Biochimie* **88**: 1773-  
615 1785

616

617 Lefevre O, Bouisset P, Germain P, Barker E, Kerlau G, Cagnat X (2003) Self-absorption correction factor  
618 applied to <sup>129</sup>I measurement by direct gamma-X spectrometry for *Fucus serratus* samples. *Nuclear*

619 *Instruments and Methods in Physics Research Section A: Accelerators, Spectrometers, Detectors and*  
620 *Associated Equipment* **506**: 173-185

621

622 Luther G, Wu J, Cullen J (1995) Redox Chemistry of Iodine – Frontier molecular orbital theory  
623 considerations. *Aquatic Chemistry* **244**: 135-155

624

625 McFiggans G, Bale CSE, Ball SM, Beames JM, Bloss WJ, Carpenter LJ, Dorsey J, Dunk R, Flynn MJ,  
626 Furneaux KL, Gallagher MW, Heard DE, Hollingsworth AM, Hornsby K, Ingham T, Jones CE, Jones RL,  
627 Kramer LJ, Langridge JM, Leblanc C, LeCrane JP, Lee JD, Leigh RJ, Longley I, Mahajan AS, Monks PS,  
628 Oetjen H, Orr-Ewing AJ, Plane JMC, Potin P, Shillings AJL, Thomas F, Von Glasow R, Wada R, Whalley  
629 LK, Whitehead JD (2010) Iodine-mediated coastal particle formation: An overview of the Reactive  
630 Halogens in the Marine boundary layer (RHAMBLe) Roscoff coastal study. *Atmospheric Chemistry and*  
631 *Physics* **10**: 2975-2999

632

633 McFiggans G, Coe H, Burgess R, Allan J, Cubison M, Alfarra MR, Saunders R, Saiz-Lopez A, Plane JMC,  
634 Wevill DJ, Carpenter LJ, Rickard AR, Monks PS (2004) Direct evidence for coastal iodine particles from  
635 *Laminaria* macroalgae - Linkage to emissions of molecular iodine. *Atmospheric Chemistry and Physics*  
636 **4**: 701

637

638 O'Dowd C, Jimenez J, Bahreini R, Flagan R, Seinfeld J, Hämerl K, Pirjola L, Kulmala M, Jennings S,  
639 Hoffmann T (2002) Marine aerosol formation from biogenic iodine emissions. *Nature* **417**: 632-636

640

641 Reyes-Umana V, Henning Z, Lee K, Barnum TP, Coates JD (2022) Genetic and phylogenetic analysis of  
642 dissimilatory iodate-reducing bacteria identifies potential niches across the world's oceans. *ISME*  
643 *Journal* **16**: 38-49

644

645 Saiz-Lopez A, Plane JMC, Baker AR, Carpenter LJ, Von Glasow R, Gómez Martín JC, McFiggans G,  
646 Saunders RW (2012) Atmospheric chemistry of iodine. *Chemical Reviews* **112**: 1773-1804

647

648 Sandell EB, Kolthoff IM (1937) Micro determination of iodine by a catalytic method. *Microchimica Acta*  
649 **1**: 9–25

650

651 Shaw TI (1959) The mechanism of iodide accumulation by the brown sea weed *Laminaria digitata*. The  
652 uptake of <sup>131</sup>I. *Proceedings of the Royal Society of London* **B151**: 356-371

653

654 Verhaeghe EF, Frayssé A, Guerquin-Kern JL, Wu TD, Devlin G, Mioskowski C, Leblanc C, Ortega R,  
655 Ambroise Y, Potin P (2008) Microchemical imaging of iodine distribution in the brown alga *Laminaria*  
656 *digitata* suggests a new mechanism for its accumulation. *Journal of Biological Inorganic Chemistry* **13**:  
657 257-269

658

659 Whitehead JD, McFiggans GB, Gallagher MW, Flynn MJ (2009) Direct linkage between tidally driven  
660 coastal ozone deposition fluxes, particle emission fluxes, and subsequent CCN formation. *Geophysical*  
661 *Research Letters* **36**

662

663 Wong G (1991) The marine geochemistry of iodine. *Reviews in Aquatic Sciences* **4**: 45-73

664  
665 Wong G (2001) Coupling iodine speciation to primary, regenerated or "new" production: a re-  
666 evaluation. *Deep-Sea Research Part I* **48**: 1459-1476

667  
668 Wong G, Cheng X-H (2001a) Dissolved organic iodine in marine waters: role in the estuarine  
669 geochemistry of iodine. *Journal of Environment Monitoring* **3**: 257-263

670  
671 Wong G, Cheng X-H (2001b) The formation of iodide in inshore waters from the photochemical  
672 decomposition of dissolved organic iodine. *Marine Chemistry* **74**: 53-64

673  
674 Zhang L (2015) Speciation Analysis and Environmental Tracer Studies of <sup>129</sup>I. PhD Thesis, Center for  
675 Nuclear Technologies, Technical University of Denmark, Roskilde, Denmark

676  
677  
678